Biodegradation (2006) 17: 389–402
DOI 10.1007/s10532-005-9009-7

Modelling MSW decomposition under landfill conditions considering hydrolytic and methanogenic inhibition

Vasily A. Vavilin[1], Susanne Jonsson[2,*], Jörgen Ejlertsson[3] & Bo H. Svensson[2]
[1]*Water Problems Institute of the Russian Academy of Sciences, 119991, Moscow, Russia;* [2]*Dept. Water and Environmental Studies, Linköping University, SE-581 83, Linköping, Sweden;* [3]*Tekniska Verken i Linköping AB, 1500SE-581 15, Linköping, Sweden (*author for correspondence: e-mail: susjo@tema.liu.se)*

Accepted 25 July 2005

Key words: aeration, anaerobic digestion, distributed model, diethyl phthalate, inhibition, methanogenesis

Abstract

A landfill typically progresses through a series of microbial degradation phases, in which hydrolysis, production and consumption of fermentation products, such as fatty acids, and methane formation play important roles. For ultimate degradation of the waste, stable methanogenic conditions have to be attained, and maintained for sufficient time. Using experimental data from 100-L landfill simulation reactors containing municipal solid waste from a residential area, a distributed model, which accounts for vertical water flow, was developed. As a first step, the waste was divided into two fractions: readily degradable and recalcitrant waste. Secondly, the general hydrolysis of the recalcitrant waste was accounted for by including a specific, well-defined chemical substance in the model that generally occurs in Municipal Solid Waste (MSW) and is hydrolysed before its further degradation to methane. For this purpose we chose diethyl phthalate and its hydrolysis product monoethyl phthalate, for which leachate data are available from the reactors. The model indicated that inhibition of the hydrolytic and methanogenic processes occurred during the acidogenic phase and that it could be overcome either by improving the chemical environment or by the complete oxidation of the inhibiting, i.e. the easily degraded, fraction of the waste. The generality of the model was confirmed by the patterns of the phthalate di- and monoester transformations obtained. The validity of the model was further confirmed using experimental data from parallel reactors, which were subjected to either leachate exchange with an already methanogenic reactor or to initial aeration to force the reactor into stable methanogenic conditions.

Introduction

Biodegradation of municipal solid waste (MSW) in landfills is a complex and variable process. Landfills develop distinctive microbial ecosystems (following the gradual infiltration of atmospheric precipitation) via complex biotic and abiotic interactions between the site and the waste (Chynoweth & Pullammanappallil 1996). After landfilling, the waste generally passes through a typical series of phases (Christensen & Kjeldsen 1989), the first of which leads to the depletion of oxygen and, thus, to a second acid fermentation phase, during which fermentation products, e.g. volatile fatty acids (VFAs) and alcohols, are produced and may appear in the leachate. The acid fermentation products decrease the pH to below 5. Since the VFAs are readily analyzed, they are often used to monitor the presence of fermentation products during anaerobic digestion. In the following text, VFA should therefore be regarded not only as estimates of VFA levels *per se*, but also as indicators of the general occurrence of fermentation products. During the third and longest period in a microbiologically active landfill, pH is neutral or slightly alkaline and methane is produced at a high and stable rate.

The different degradation processes are not definitive, since dynamic variations in the environmental conditions result in changes in their distribution and rates within the landfill. For example, during certain circumstances, the acid-formers may outgrow methane-formers, which can lead to acidification and cessation of the anaerobic digestion process (Barlaz et al. 1989). Vavilin et al. (2003) have formerly modelled the conditions under which there is virtually complete VFA conversion to methane in the methanogenic zones, based on data acquired from experiments where waste was incubated in 2-l reactors and the pH of the recirculated leachates was adjusted to maintain methanogenic conditions. This resulted in a distributed model of MSW decomposition in a 1-D bioreactor with leachate recirculation and pH adjustment, which could be used to analyze the balance between the rates of polymer hydrolysis and methanogenesis.

The degradation phases that occur in landfills, as described above, have also been simulated in landfill-simulating reactors, where the timescale is months to years rather than decades (Ejlertsson et al. 2003; Lagerkvist & Chen 1992; Pohland et al. 1992; Stegmann 1981). The acidic stage can be avoided by initial aeration allowing methanogenesis to develop when the aeration is switched off. Ejlertsson et al. (2003) investigated 100-l landfill-simulating reactors with MSW under both methanogenic conditions (initiated by aeration) and acidogenic conditions. After three years of stable acidity, the acidogenic reactor was forced into neutral, methane-forming conditions by exchanging leachates between the two reactors. The set up of these landfill-simulating reactors and their operational parameters, including the aeration procedures, should facilitate studies that could be used to expand the previous modelling efforts, as described in Vavilin et al. (2003). In the present study, the complex processes occurring vertically in landfills were modelled by developing a distributed one-dimensional (1-D) model, which accounts for a vertical water flow. By this, the fermentation and methane formation processes were studied. The model includes retardation of the overall degradation of MSW due to the effect of formation of fermentation products with an emphasis on those causing acidification. Experimental data from 100-l landfill-simulation reactors (Ejlertsson et al., 2003) were used for developing the model. Diethyl phthalate (DEP) was used as a reference substance (by monitoring its conversion to the corresponding monoester, monoethyl phthalate; MEP) as an indicator of the hydrolytic activities of the system towards the bulk waste. The water-soluble DEP is a diester and its hydrolysis to MEP and phthalic acid under different landfill conditions has been confirmed in previous studies (Ejlertsson et al. 1996a,b; Jonsson et al. 2003a), in which DEP was degraded via hydrolysis to the monoester and phthalic acid (and finally to methane and carbon dioxide) under methanogenic conditions, but resisted degradation when acid conditions prevailed. Ultimate cleavage due to chemical hydrolysis of DEP during landfill conditions is likely negligible, since the halftime for DEP is 8.8 years at pH 7. The phthalate monoesters are even more resistant to chemical hydrolysis than their corresponding diesters (Wolfe et al. 1980).

Methods

Experimental studies used for developing and calibrating the model

Data from two 100-l landfill simulation reactors, called LiU1 and LiU3, were used to develop and calibrate the 1-D model. The reactors were set up to simulate the ageing sequence of a landfill. For details on the waste used, operation and reactor performance, see Ejlertsson et al. (2003). A detailed description of the experimental measurements of phthalate concentrations in the leachates is presented in Jonsson et al. (2003a). The reactor performance and selected results from the phthalate analyses are briefly described below.

Each of the reactors contained MSW, collected from a residential area in Sweden. As well as solid organic materials, such waste tends to contain the phthalate we intended to use as model substance (Jonsson et al. 2003a,b,c). Water was added to give a moisture content of 65% (wet weight). Due to rapid fermentation, acidogenic conditions were established within a few days after filling and closing the reactors. Reactor LiU3 was operated under acidogenic condition (as confirmed by VFA analyses and pH measurements), while LiU1 was methanogenic (as confirmed by analysing the methane content of the gas produced). In order to ensure that conditions were methanogenic and avoid acidification of the latter, it was continuously aerated for the first three weeks following day 4, and then twice a week until the end of week 17. Fluctuating concentrations of VFA, DEP and MEP were observed in the leachate due to the alternately aerobic and anaerobic conditions (Figure 3). After 17 weeks, when gas production stabilised, aeration was stopped and the waste became anaerobic and methanogenic, resulting in a steady pH at *ca.* 7 and no accumulation of VFA. Over the following year the MEP generated during the aeration period decreased to below the detection limit (1 μg l^{-1}). Leachates from the acidogenic LiU3 were withdrawn (3 l week^{-1}) and replaced by tap water to simulate precipitation (100 l in total). The dilution procedure continued from week 18 to week 51 and was monitored by measuring inorganic halides in the leachates (Ejlertsson et al. 2003). During the dilution, the VFA concentration decreased ten-fold, although the pH level remained at *ca.* 5.5. Termination of the water addition simulated the covering of a landfill. After 148 weeks of operation, the acidogenic reactor, LiU3, was slowly made methanogenic by exchanging one litre of leachate once a week with leachate from LiU1 until week 169. The exchange of leachate was terminated when methanogenic conditions were established and biogas was generated from the waste in LiU3 at a steady rate.

Two other reactors: LiU2 (a parallel to LiU1) and LiU4 (a parallel to LiU3), were included in the study for validation of the model. However, the parallel reactors contained 12.5% less MSW, and were supplemented with a corresponding amount of waste fractions containing potential pollutants (e.g. plasticizer-containing plastics, freon-blown insulation and materials containing flame-retardants), which hampered the development of the degradation phases in them (Ejlertsson et al., 2003). Consequently, the methanogenic activity in LiU2 was probably weaker than expected after the aeration period, and a longer period of leachate exchange was required for stable production of biogas to begin in LiU4 (until week 228 compared to week 169 for LiU3).

The model

The transformations considered in the kinetic analysis of the distributed 1-D reactor model are presented in Figure 1. In order to make the model manageable and interpretable we made several simplifying assumptions about the decomposition processes of solids. First, the bulk organic waste was divided into two fractions, according to its

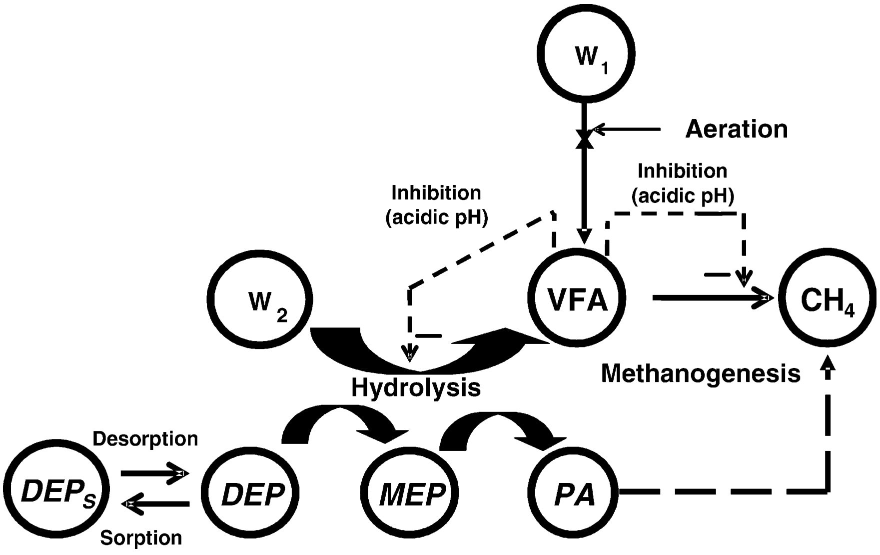

Figure 1. Scheme of co-digestion of the different fractions of MSW and transformation of the dissolved diethyl phthalate (DEP) to its monoester (MEP and phthalic acid (PA). Other abbreviations: PDs, sorbed PD; W1, readily degradable waste; W2, recalcitrant waste; VFA, volatile fatty acids.

potential degradability: readily degradable and recalcitrant. Second, all transformation processes involving the conversion of VFA to methane were lumped together as a single step in the model. Also, methane formation included both hydrogenotrophic and acetoclastic methanogenesis. Third, the anaerobic digestion of MSW was considered to be a two-stage process, i.e. acidogenic and methanogenic, and the fermentation products were regarded as a single intermediate, namely VFA, which serves as the precursor for methane production. The degradation of the two waste fractions, as well as DEP and MEP, was supposed to follow first-order kinetics, in accordance with earlier studies (Batstone et al. 2002; Gavala et al. 2003) To describe methanogenesis, Monod kinetics for biomass growth of methanogenic microorganisms was used (cf. Batstone et al. 2002). Hydrolysis/acidogenesis and methanogenesis were the rate-limiting steps of the overall anaerobic MSW digestion process.

The original data showed a delay in both methanogenesis and phthalate degradation under acidic conditions (LiU3). Therefore, it was assumed that inhibition of the hydrolysis of recalcitrant waste, DEP and MEP as well as of methanogenesis took place.

Monod kinetic approaches provide convenient ways to deal with inhibition, but their use imply the involvement of organisms. Therefore, the methanogenic activities in the reactors and leachates were approximated to certain concentration equivalents of methanogens and Monod kinetics were then applied. Methane formation from phthalate transformation was not taken into account because the total amount of phthalate was negligible in comparison with the initial amount of MSW. In order to model the hydrolysis of MSW-related DEP, the phthalate needs to be exposed to the hydrolytic activity in the liquid phase. A release of DEP from the waste matrix was therefore introduced in the model (1). MEP is produced in the liquid phase and its sorption to the waste is negligible because of its high solubility (> 3.2 g l^{-1}; Jonsson & Baun 2003).

Advection components of processes affecting dissolved VFA, protons, DEP, MEP, were considered to be entirely due to the water flow. The methanogenic microorganisms were considered to only partly be transferred by the liquid flow. All biogas formed was considered to be present in the head-space gaseous phase. Initial carbon dioxide formation during the hydrolysis/acidogenesis was not accounted for by the model. The rate of methanogesis was included as the driving force for the total degradation processes, and simulated by modelling the methanogenically active populations in the reactors.

The following system of nine parabolic partial differential equations, in which Z is the vertical coordinate of the 1-D reactor, where $Z = 0$ and $Z = 1$ are the top and bottom of the reactor, respectively, was used for our modelling purposes:

$$
\begin{aligned}
\frac{\partial W_1}{\partial t} &= -\, k_{h1}\, W_1 \,, \\
\frac{\partial W_2}{\partial t} &= -\, k_{h2} f_1(I)\, W_2 \,, \\
\frac{\partial \mathrm{VFA}}{\partial t} &= D_{\mathrm{VFA}} \frac{\partial^2 \mathrm{VFA}}{\partial Z^2} - q \frac{\partial \mathrm{VFA}}{\partial Z} \\
&\quad + \chi_1\, k_{h1}\, W_1 + \chi_2\, k_{h2} f_1(I)\, W_2 \\
&\quad - \rho_m f_2(I) \frac{B_M \mathrm{VFA}}{K_{\mathrm{VFA}} + \mathrm{VFA}} \,, \\
\frac{\partial B_M}{\partial t} &= D_B \frac{\partial^2 B_M}{\partial Z^2} - q\alpha \frac{\partial B_M}{\partial Z} \\
&\quad + Y \rho_m f_2(I) \frac{B_M \mathrm{VFA}}{K_{\mathrm{VFA}} + \mathrm{VFA}} - k_d B_M \,, \\
\frac{\partial \mathrm{CH}_4}{\partial t} &= (1 - Y) \rho_m f_2(I) \frac{B_M \mathrm{VFA}}{K_{\mathrm{VFA}} + \mathrm{VFA}}, \\
\frac{\partial H}{\partial t} &= D_H \frac{\partial^2 H}{\partial Z^2} - q \frac{\partial H}{\partial Z} \\
&\quad - b f_2(I) \frac{B_M \mathrm{VFA}}{K_{\mathrm{VFA}} + \mathrm{VFA}} H, \qquad (1) \\
\frac{\partial \mathrm{DEP}_s}{\partial t} &= -\, k_1\, \mathrm{DEP}_s + k_2\, \mathrm{DEP} \,, \\
\frac{\partial \mathrm{DEP}}{\partial t} &= D_{\mathrm{DEP}} \frac{\partial^2 \mathrm{DEP}}{\partial Z^2} - q \frac{\partial \mathrm{DEP}}{\partial Z} \\
&\quad - k_2\, \mathrm{DEP} + k_1\, \mathrm{DEP}_s - k_{h3} f_3(I)\, \mathrm{DEP}, \\
\frac{\partial \mathrm{MEP}}{\partial t} &= D_{\mathrm{MEP}} \frac{\partial^2 \mathrm{MEP}}{\partial Z^2} - q \frac{\partial \mathrm{MEP}}{\partial Z} \\
&\quad + k_{h3} f_3(I)\, \mathrm{DEP} - k_{h4} f_3(I)\, \mathrm{MEP},
\end{aligned}
$$

where W_1, W_2, VFA, H are readily degradable and recalcitrant solid wastes, total VFA and proton concentrations, respectively; CH_4 is the amount of methane; DEP, MEP are dissolved di- and mono phthalate ester concentrations, respectively; DEP_s is sorbed DEP; B_M is the methanogenic biomass concentration; $f_1(I)$, $f_2(I)$, $f_3(I)$ are dimensionless inhibiting functions; t is time ($0 \leq t \leq +\infty$); k_{h1}, k_{h2}, k_{h3} and k_{h4} are the corresponding first-order hydrolysis rate constants of readily degradable waste, recalcitrant waste, DEP and MEP, respectively; ρ_{m1} is the maximum specific rates of VFA utilization; k_d is the specific biomass decay coefficient for methanogens; α is the part of the methanogenic biomass that is transferred by the liquid flow; k_1 and k_2 are the desorption and sorption constants for DEP, respectively; χ_1, χ_2, are the stoichiometric coefficients of readily and degradable recalcitrant waste, respectively; b is the rate constant for the decrease of proton concentration during methanogenesis; K_{VFA} is the half-saturation constants for VFA utilization; Y is the corresponding methanogenic biomass yield coefficient; q is the volumetric liquid flow rate per unit surface area (specific liquid flow rate); D_{VFA}, D_H, D_{DEP} and D_{MEP}, are the diffusion coefficients for VFA, protons, DEP, and MEP, respectively; D_{BM} is the diffusion coefficient for methanogens; and L is the reactor height. The nomenclature, initial and parameter values are shown in Table 1.

Under initial conditions, all variables were assumed to be uniformly distributed in the reactor over the vertical coordinate Z. However, due to differences in the treatments and the naturally developing processes, the following boundary conditions were introduced in the model: changes of parameter concentrations during naturally developing processes throughout the study (eq. 2), changes of parameter concentrations due to dilution (eq.3 and 4) and changes of concentrations due to leachate exchange between the reactors (eq.4).

$$\frac{\partial c}{\partial Z} = 0(z=0); \quad \frac{\partial c}{\partial Z} = 0(z=L)$$
$$\text{weeks}: 1-17, 53-143, 170-250 \tag{2}$$

$$\frac{\partial c}{\partial Z} = \frac{q_1}{D}(0-c)(z=0);$$
$$\frac{\partial c}{\partial Z} = 0(z=L) \quad \text{weeks}: 18-52 \tag{3}$$

$$\frac{\partial B_M}{\partial Z} = \frac{\alpha q_1}{D}(0-B_M)(z=0);$$
$$\frac{\partial B_M}{\partial Z} = 0(z=L) \quad \text{weeks}: 18-52 \tag{4}$$

$$\frac{\partial c}{\partial Z} = \frac{q_2}{D}(c^* - c)(z=0);$$
$$\frac{\partial c}{\partial Z} = 0(z=L) \quad \text{weeks}: 144-169 \tag{5}$$

$$\frac{\partial B_M}{\partial Z} = \frac{\alpha q_2}{D}(B_M^* - B_M)(z=0);$$
$$\frac{\partial B_M}{\partial Z} = 0(z=L) \quad \text{weeks}: 144-169 \tag{6}$$

In eq. (2), c represents all variables of the model (1). In eqs. (3, 5) c represents the VFA, H, DEP and MEP concentrations, while c^* and B_M^* represents the corresponding concentrations in the incoming leachate. The final values of variables for one stage were used as the initial values for the next stage.

Water was not considered as a limiting factor, because the waste was assumed to be water saturated, allowing the reactions to occur independently of the water content. It has been suggested that the reduction in hydraulic conductivity in the porous waste medium due to settling of the waste should be taken into account in full-scale studies of microbial decomposition of landfilled MSW (Vavilin 2003). However, this was not considered to be important for the 100-l reactors used in this study, so it was not included in the model.

Inhibition. In order to explain the delay in the establishment of methanogenic activity in the initially acidogenic reactor, two types of inhibition functions $f_i(I)$ were introduced in the model (1). First, we assumed that the inhibition was either directly or indirectly related to the proton concentration. To model a direct relationship, a reduction in the proton concentration from $10^{-5.5}$ to 10^{-7} moles l^{-1} was considered, since the pH level in the original acidogenic reactor changed from acid (5.5) to circumneutral (7) during the development from acidogenic to methanogenic conditions. According to the resulting model, the rate of the decrease in proton concentration is proportional to the increase in the rate of methanogenesis. To model an indirect relationship, it was assumed that the inhibition was correlated with the concentration of the non-ionized form of VFA (HVFA). The total concentration of VFA reported in Ejlertsson et al. (2003) is the sum of non-ionized and ionized forms of VFA, i.e. $[\mathrm{VFA}] = [\mathrm{HVFA}] + [\mathrm{VFA}^-]$.

Table 1. The model parameters

Abbreviation	Description	Parameter values	Initial values
α	the part of the methanogenic biomass transferred by the liquid flow	0.1	
a, n	constants in the inhibiting function (7)	4.8 resp. 14	
b	constant for the decrease of proton concentration during methanogenesis	0.23 l week^{-1} g^{-1}	
B_M	conc. of methanogenic biomass		0.01 g l^{-1}
B_M*	conc. of methanogenic biomass in the incoming leachate	0.5 g l^{-1}	
c	all variables in the model (1)		
c*	conc. of component c in the incoming leachate		
CH_4	volume of methane released		0 l
dCH_4/dt	methane production rate		
DEP, MEP	conc. of DEP and MEP, resp.		0.01 and 0 mg l^{-1}, resp.
DEP$_s$	conc. of sorbed DEP		7 mg l^{-1}
DEP*, MEP*	DEP and MEP conc, respectively in the incoming leachate	0.001 and 0.001 *mg l*$^{-1}$, resp.	
D_{BM}	diffusion coeff. for methanogens	0.001 l^2 week^{-1}	
D_{DEP}, D_{MEP}	diffusion coeff. for DEP and MEP, resp.	0.001 l^2 week^{-1}	
D_{VFA}	diffusion coeff. for VFA	0.001 l^2 week^{-1}	
f_1(I)	inhibiting function for hydrolysis		
f_2(I)	inhibiting function for methanogenesis		
f(pH)	inhibition function with proton conc. as inhibiting agent		
f(HVFA)	inhibition function with non-ionized VFA conc. as inhibiting agent		
I	inhibitor		
H	proton conc.		10$^{-5.5}$ g l^{-1}
H*	proton conc. in the incoming leachate		10$^{-7.0}$ g l^{-1}
K_i	inhibition coeff. in function (8)		
K_1	inhibition constant of hydrolysis	0.04 g l^{-1}	
K_2	inhibition constant of methanogenesis	0.065 g l^{-1}	
K_3	inhibition constant of DEP and MEP	0.02 g l^{-1}	
K_{VFA}	half-saturation constant for VFA utilization	3.5 g l^{-1}	
k_d	decay coeff. of methanogens	0.005 week^{-1}	
k_{h1}, k_{h2}	first-order hydrolysis rate constants for readily degradable and recalcitrant MSW, resp.	0.58 and 0.049 week^{-1}, resp.	
k_{h3}, k_{h4}	first-order hydrolysis rate constants for DEP and MEP, resp	0.23 and 0,084 week^{-1} resp.	
k_{ox1}	first-order rate constants of VFA oxidation	1 week^{-1}	
k_{ox2}	First-order rate constant of DEP oxidation to MEP	5 week^{-1}	
k_{ox3}	first-order rate constants of MEP oxidation	0.1 week^{-1}	
k_1, k_2	first-order desorption and sorption rate constants for diethyl phthalates	0.13 and 0.50 week^{-1}, resp.	
L	cylinder reactor height	0.80 m	
q	volumetric liquid flow rate per unit surface area (specific liquid flow rate)		
q_1, q_2	specific liquid flow rate during the periods of dilution and leachate addition, resp.	0.09 and 0.03 l week^{-1}, resp.	
ρ_{VFA}, ρ_{DEP}, ρ_{MEP}	oxidation rates of VFA, DEP and MEP, resp.		
ρ_m	maximum specific rate of VFA utilization	15.4 week g g^{-1}	
t	time	$0 \leq t \leq +\infty$	
VFA	VFA conc.		4 g l^{-1}

Table 1. Continued

Abbreviation	Description	Parameter values	Initial values
VFA*	VFA conc. in the incoming leachate during leachate exchange	0.001 g l^{-1}	
W_1	conc. of readily degradable MSW		70 g l^{-1}
W_2	conc. of recalcitrant MSW		280 g l^{-1}
Z	vertical coordinate (0 = top, 1 = bottom of the reactor)	$0 \leq Z \leq L$	
Y	biomass yield coeff. for methanogens	0.1 g g^{-1}	
χ_1, χ_2	stoichiometric coeffs. of the transformation of readily degradable and recalcitrant waste to VFA, resp.	0.42 and 0.6, resp.	

The dimensionless functions $f_i(I)$ describe the inhibition of hydrolysis of recalcitrant waste (W_2) and phthalates (DEP and MEP), and of methanogenesis, i.e. the ultimate degradation of organic waste (including phthalates) to biogas:

$$f_i(\mathrm{pH}) = \frac{(\mathrm{pH} - a)^n}{1 + (\mathrm{pH} - a)^n} \tag{7}$$

where pH $= -\lg[\mathrm{H}^+]$, a and n are constants, and i = 1 (hydrolysis of recalcitrant waste), 2 (methanogenesis), 3 (hydrolysis of DEP and MEP) or:

$$f_i(\mathrm{HVFA}) = \frac{1}{1 + \left\{\dfrac{\mathrm{VFA}}{K_i(1 + K_a/H)}\right\}^2} \tag{8}$$

where K_a = 2.0×10^{-5} is the dissociation constant for VFA, and K_i is the inhibition coefficient. The inhibiting functions (8) used in the model (1) is shown in Figure 2.

The possible inhibition from the extra pollutants present in LiU4, is not elaborated on. This is just represented by lower hydrolytic constants and a response delay in LiU4 (44 weeks), occurring from the start of the leachate exchange.

Aeration. Since LiU1 and LiU2 were aerated periodically during the first period, oxidation of VFA, DEP and MEP was introduced in the model (1) in the form of simple first-order reactions:

$$\rho_{\mathrm{VFA}} = -k_{ox1}\mathrm{VFA}, \quad \rho_{\mathrm{DEP}} = -k_{ox2}\mathrm{DEP}, \quad \rho_{\mathrm{MEP}} = k_{ox2}\mathrm{DEP} - k_{ox3}\mathrm{MEP} \tag{9}$$

where ρ_{VFA}, ρ_{DEP}, ρ_{MEP} are the oxidation rates of VFA, DEP and MEP, respectively, and $k_{ox1}, k_{ox2}, k_{ox3}$ are their corresponding first-order rate constants.

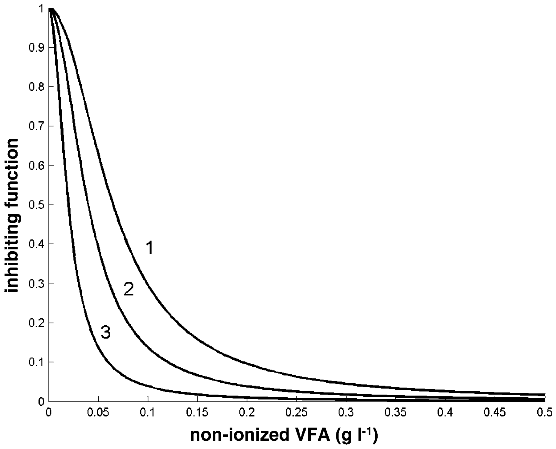

Figure 2. The dimensionless functions of inhibition by non-ionized VFAs (*f*(HVFA)) of methanogenesis (1), hydrolysis of recalcitrant MSW (2) and phthalate hydrolysis (3).

All numerical simulations were performed using MATLAB software. Visual comparison between experimental data and the simulations made it possible to arrive at values of coefficients at which the sum of the differences between the observed and predicted values of model variables were near at a minimum. Since the complexity of the model makes it extremely difficult to perform an identifiable study, it is not possible to ensure the uniqueness for the set of estimated parameters. However, the simulations have been done after trying many sets of parameters, choosing values with physical and biological sense, and ensuring that, if there are other sets of parameter values, these will be of the same order of magnitude.

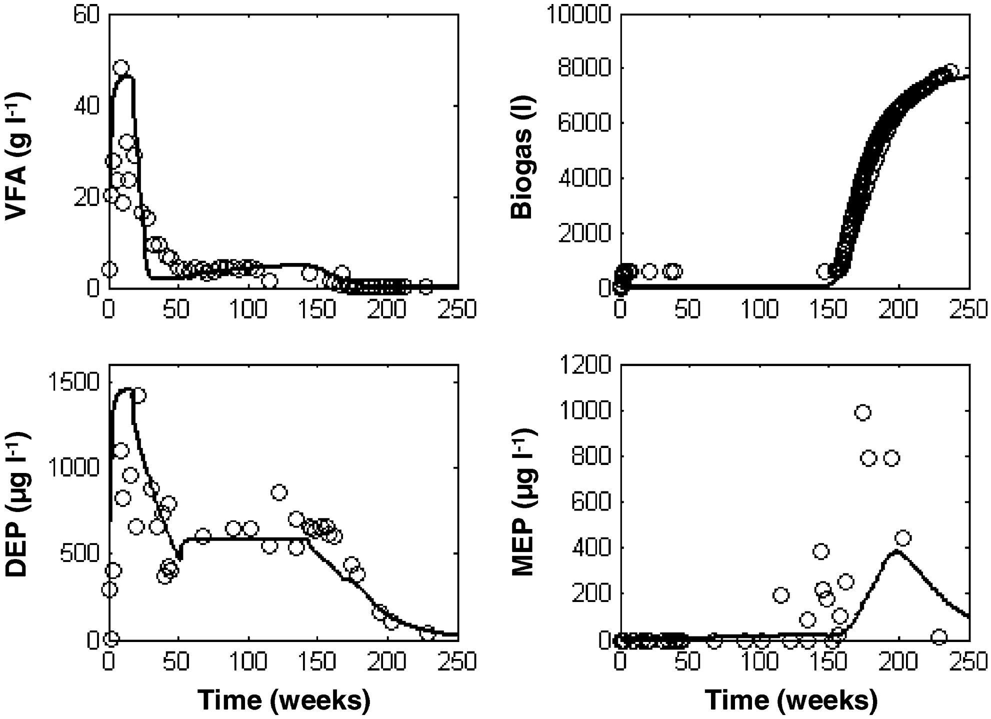

Figure 3. Time profiles of VFA, DEP and MEP concentrations in the leachate averaged over the reactor volume, and the total biogas volume released in the initially acidogenic reactor, LiU3. The circles represent values measured in the actual reactor and the lines are results obtained using the model.

Results and discussion

Differences in the operation and performance of the two MSW reactors made it possible to use experimental data obtained from LiU1 to validate the inhibition theory, imposed by the experimental data of LiU3. Bearing in mind that the same basic set of parameters was used for both reactors, the fit of the model to the experimental data is satisfactory. It should be mentioned that the periods of intermittent aeration and leachate exchange, which generated fluctuations in the experimental concentrations due to the relatively rapid changes in various degradation processes (aerobic–anaerobic and acidogenic–methanogenic), were modelled as continuous processes. Therefore, the model was not intended or expected to give a precise fit to individual experimental data points during these periods. Instead, the fit of the model to the average experimental data was the key validation criterion during these periods.

Degradation of the bulk waste under landfill conditions

According to the model, VFA accumulated in the leachate before the dilution period of the originally acidogenic reactor (LiU3) due to hydrolysis and fermentation of the easily degradable waste (Figure 3). The hydrolysis rate coefficients of readily degradable (k_{h1}) and recalcitrant (k_{h2}) wastes were 0.58 week^{-1} = 0.08 day^{-1} and 0.049 week^{-1} = 0.007 day^{-1}, respectively. Thus, the former was hydrolysed about 10 times more rapidly than the latter. The former value was in the same range, but the latter value was much lower than the corresponding values presented by Vavilin et al. (2004), 0.02 and 0.06 day^{-1}, which dealt with the grey waste fraction of MSW. The large difference in hydrolysis rate of the recalcitrant materials is likely due to (i) the different sizes of the reactors, i.e. 1.5 vs 100 l for the grey waste and the MSW in this study, respectively; (ii) the small grey waste reactors were run at higher temperature (35°C, compared to the reactors, which were stored at 30°C); and (iii) the grey waste was inoculated with 0.5 l of municipal sewage sludge, which, according to the discussion above, would secure conditions promoting an efficient hydrolysis. The initial rate of VFA accumulation was derived from the former coefficient (k_{h1}). Furthermore, the VFA concentrations decreased during the dilution (weeks 18–52) in accordance with the dilution rates.

After termination of the dilution, the VFA concentration increased slightly as a result of residual hydrolysis and fermentation of readily degradable waste. In the subsequent acidogenic steady state, in which there was a relatively long period of nearly constant VFA and proton concentrations, no further degradation occurred. The model shows that both methanogenesis and hydrolysis were inhibited. The inhibition remained although the VFA occurred at a relatively low concentration, i.e. *ca.* 5 g l^{-1}, which is less in relation to the levels often referred to as inhibiting anaerobic digestion (about 30 g l^{-1}: Vavilin et al. 2004; Brummeler et al. 1991). When leachate exchange between the two reactors took place, during weeks 144–169, methanogenesis commenced in the formerly acid reactor (LiU3). This allowed successive syntrophic degradation of fermentation products, as shown by the decrease in the VFA, which in turn caused an increase in pH and an accelerated methane formation. According to the model, the transfer of methanogenically active leachate thus led to enhanced hydrolysis of the recalcitrant waste fraction, which in turn resulted in biogas production (Figure 3). The change in VFA concentrations in the reactor during dilution and methanogenic degradation of the acids was predicted by the model by a concentration front of acids, expressed as VFA passing through the reactor (Figure 4). The model suggests that the inhibition of hydrolysis of recalcitrant MSW ceased at the top of the reactor, where methanogenesis developed firstly and then propagated throughout to the bottom. Unfortunately, lack of experimental data made it impossible to confirm the modelled fronts.

Proton dynamics

The responses of the model, and the accuracy with which it simulated the results obtained by Ejlertsson

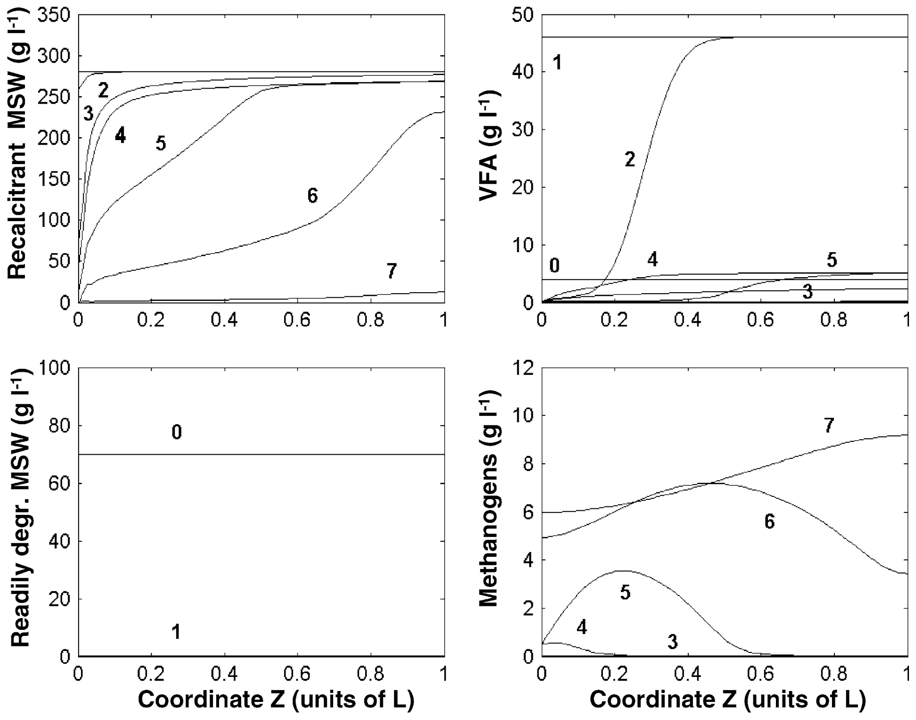

Figure 4. Profiles throughout the coordinate Z of W_1, W_2, VFA, and B_M concentrations in the initially acidogenic reactor, LiU3, at 0 (0), 18 (1), 21 (2), 50 (3), 149 (4), 164 (5), 190 (6), and 250 (7) weeks of incubation.

et al. (2003) and Jonsson et al. (2003), were similar regardless of whether the inhibition was assumed to be mediated directly by pH or by non-ionized VFA. Therefore, we conclude that the inhibition was directly and/or indirectly related to the proton concentration. Despite a substantial reduction of the VFA concentrations during the dilution period in LiU3, the pH value remained constant at about 5.5, implying that a simultaneous decrease in the concentration of other cations (N) occurred during the dilution. Cations influence the concentrations of proton and non-ionized acids via the following ionic balance: $[\mathrm{OH}^-] + [\mathrm{VFA}^-] \equiv [N^+] + [H^+]$, or for circum-neutral conditions: $[\mathrm{VFA}^-] \approx [N^+]$. This relationship has been previously used by Vavilin et al. (2003). Consequently, the concentration of non-ionized VFA (HVFA) is also influenced by the cation concentration, since $[\mathrm{HVFA}] \leftrightarrow [\mathrm{VFA}^-]+[\mathrm{H}^+]$.

The dissociation constant used in the inhibiting function (8), presumed to be caused by VFA, correspond to a pK_a of 4.70, which is somewhat lower than that of acetic acid, i.e. 4.78. This clearly indicates that other acids are generated during the degradation of MSW than the volatile aliphatic mono-acids (C_2–C_6), which were included in the experimental analysis (Ejlertsson et al. 2003). Acids that may be produced as fermentation products and have a lower pK_a than acetic acid include other aliphatic acids such as α-hydroxy carboxylic acids, e.g. as lactic acid ($pK_a = 3.08$), dicarboxylic acids, e.g. oxalic acid ($pK_a = 4.19$), and also aromatic acids, e.g. benzoic acid ($pK_a = 4.19$). The possibility that other aromatic acids, e.g. cresols, are also produced cannot be excluded. It should be noted that the pK_a for cresols is ≥10, so they are probably more or less completely non-ionized at any pH lower than 8. Unfortunately, the concentrations of cresols in LiU3 are unknown.

The wide range of possible proton sources, including inorganic buffers, and lack of corresponding data, made it difficult to accurately model the pH. However, the model (1) accounted for the effects of leachate exchange and an increase in pH was observed in the reactors (Figure 5). If the leachate exchange, in which a circum-neutral leachate was introduced, was the only pH-increasing factor, pH should have increased but stayed at *ca.* 6.4 (case 2 in Figure 5). By including the methanogenic consumption of VFA, the modelled increase in pH reached the final levels that were experimentally observed (i.e. *ca.* 6.8; case 1 in Figure 5).

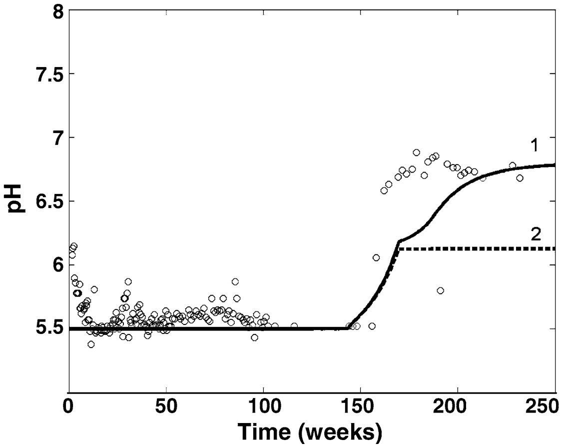

Figure 5. Time profiles of pH levels in reactor, LiU3. Weeks 0–148 were acidogenic, during weeks 149–169 methanogenic leachate was periodically introduced, while the last period was at stable methanogenic conditions. Symbols refer to experimental data and line to model prediction at $b = 0.23$ l week^{-1}g^{-1} (1) and $b = 0$ (2).

Effects of initial aeration

Several reports have indicated that the initial acidic phase can be avoided, or at least minimised, by exposing the waste to air to an appropriate extent (Lagerkvist 2003). The modelling presented here shows that further degradation of the MSW is inhibited as long as there is enough readily degradable waste to generate sufficient inhibitory fermentation products. Methane production began immediately after the aeration period (Figure 6), when both VFA and proton concentrations had decreased substantially. This shows that neither hydrolysis nor methanogenesis was inhibited when VFA was eliminated and the pH was approximately neutral.

Since a gas leakage occurred in the reactor that was aerated initially, LiU1, the modelled biogas accumulation cannot be confirmed by experimental measurements. However, we believe that the modelled pattern reflects true patterns of the gas production that occurred in LiU1 after abatement of the acids, since measured values of a parallel

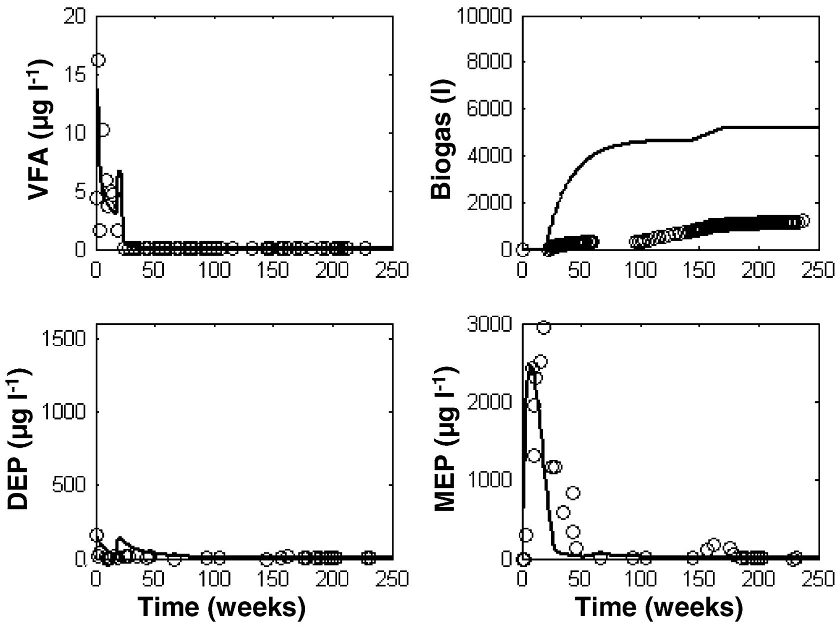

Figure 6. Time profiles of VFA, DEP and MEP concentrations in the leachate averaged over the reactor volume, and the total biogas volume released in the methanogenic reactor, LiU1, which was initially aerated during weeks 0–17. The circles represent values measured in the actual reactor and the lines are results obtained using the model.

reactor (LiU2) were more close to the modelled than were data from LiU1 (data not shown).

Phthalate transformations

The general hydrolysis of recalcitrant waste was exemplified by modelling the occurrence of DEP and its hydrolysed product, MEP, in the leachate. In order to model the hydrolysis of MSW-related DEP, the phthalate needs to be exposed to the hydrolytic agents in the liquid phase. The desorption and adsorption rate constants for DEP were $k_1 = 0.13$ and $k_2 = 0.50$, respectively, in order to model the concentration levels observed by Jonsson et al. (2003a). The model dynamics of DEP and MEP and experimental data from LiU3 are presented in Figure 3. During the dilution period (weeks 18–52), DEP concentrations decreased in accordance with the measured dilution rates. After termination of the dilution, the DEP concentration slightly increased as a result of further desorption of the DEP remaining in the waste matrix. According to the model, only non-transformal physico-chemical processes (i.e. desorption and adsorption) affected DEP up to this stage. Thus, DEP was not hydrolysed during the acidogenic phase. Hydrolysis of DEP, and further hydrolysis of MEP, occurred only during the methanogenic period.

During the aeration period in LiU1, the released amounts of DEP were efficiently hydrolysed to MEP, which was further hydrolysed (Figure 6). Aerobic degradation of DEP is well known (Saeger & Tucker 1973; references in Staples et al. 1997). During the first part of the following methanogenic period, non-oxidized MEP (remaining from the aeration period) was further hydrolysed without any lag-phase.

There was a 2.7-fold difference in the hydrolysis rate coefficients for DEP and MEP ($k_{h3} = 0.23$ and, $k_{h4} = 0.084$ week^{-1}, respectively). The lower hydrolytic rate of the monoester compared to the diester resulted in a temporary occurrence of the monoester during the initial phase of degradation of the more recalcitrant waste in LiU3 and during the aeration period in LiU1 (Figures 3 and 6 respectively). This indicates that the capacity for hydrolysis of the organic material of the MSW depends on the type of chemical bonds to be hydrolysed and the characteristics of the waste organic compound. However, in order to elucidate the range of hydrolytic rates, other types of hydrolysable compounds have to be investigated.

The modelled vertical distribution of DEP and MEP in LiU3 describes the ongoing transformations in the reactor (Figure 7). The correctness of the modelled distribution is proved by its prediction of a high concentration front of MEP close to the bottom of the reactor at week 190 (Figure 3), coinciding with a transient accumulation of MEP observed in the leachate during the same period by Jonsson et al. (2003a).

Model validation

A parallel reactor to LiU3 (LiU4, see Ejlertsson et al. (2003) for details) was used to validate the model. The model dynamics in the LiU4 reactor and experimental data are presented in Figure 8, which show that the basic model framework had a strong capacity to encompass the performance of this reactor in relation to the experimentally measured values. However, since LiU4 contained less MSW than LiU3, the initial concentrations of readily degradable waste, recalcitrant waste and DEP were lowered to 40 g l^{-1}, 240 g l^{-1} and 5 mg l^{-1}, respectively. The hydrolytic rate constants for the recalcitrant waste and the maximum specific rate of VFA consumption were k_{h2} = 0.021 $week^{-1}$ and ρ_{h2} = 7.0 g $week^{-1}$ g^{-1}, respectively, which are about half the rates of LiU3. All other model coefficients were the same as for LiU3.

Most sensitive parameters

The model (1) includes a high number of model coefficients (Table 1), which enabled the description of five sequential regimes (see eqs. 2–6), including periods of continuous flow of incoming water (simulating artificial precipitation) or methanogenic leachate (simulating leachate transport through a landfill) through the reactor. The inhibition of hydrolysis of recalcitrant MSW, methanogenesis and phthalate transformation by non-ionized VFA and/or proton concentration (pH) were identified as being the most important factors affecting the system dynamics. The specific maximum growth rate of the methanogens (μ_m) given by the model was $\mu_m = Y\rho_{m1} = 0.1$ g $g^{-1} \times$ 15.4 $week^{-1}$g g^{-1} = 1.54 $week^{-1}$ = 0.22 day^{-1}. This value is within the range of μ_m values

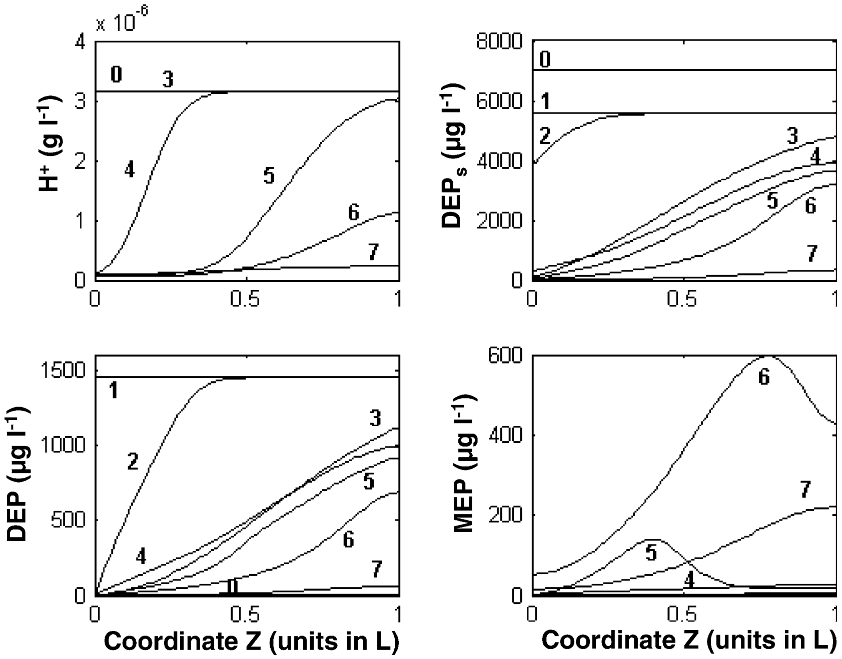

Figure 7. Profiles throughout the coordinate *Z* of proton, DEPs, DEP, and MEP concentrations in the initially acidogenic reactor, LiU3, at 0 (0), 18 (1), 21 (2), 50 (3), 149 (4), 164 (5), 190 (6), and 250 (7) weeks of incubation.

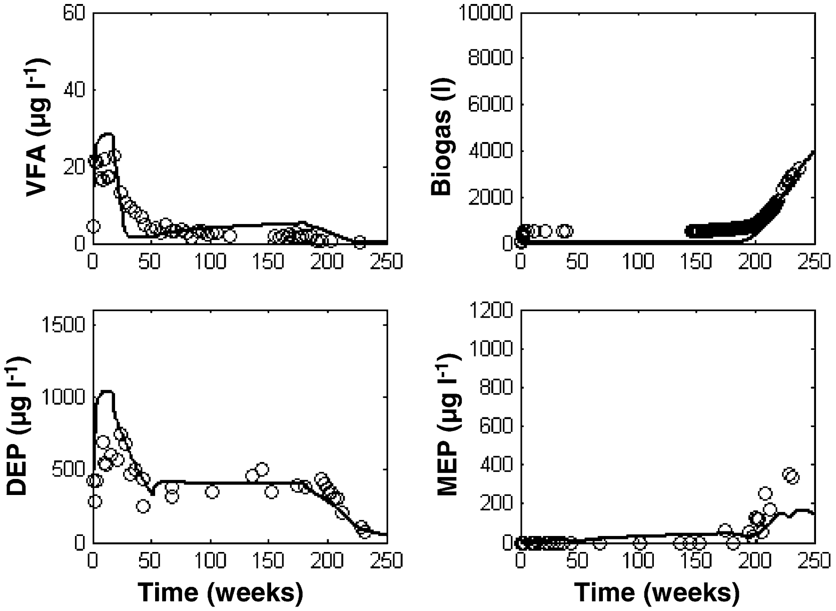

Figure 8. Time profiles of VFA, DEP and MEP concentrations in the leachate averaged over the reactor volume, and the total biogas volume released in reactor LiU4. The circles represent values measured in the actual reactor and the lines are results obtained using the model.

presented in the literature for acetoclastic methanogens (0.1–1.4 day^{-1}; Batstone et al. 2002) thus, providing confidence in the model's construction and performance. The cumulative rates of biogas formation were closely related to the maximum specific rate of VFA utilization (ρ_{m1}). However, according to the inhibiting functions presented in Figure 2, the hydrolysis of recalcitrant waste was the rate-limiting process. Thus, the biogas accumulation rate significantly depends on the value of first-order hydrolysis rate constants of recalcitrant MSW (k_{h2}) rather than the maximum specific rate of VFA utilization (ρ_{m1}). However, the methanogenic activity in the reactor was the driving force for the total degradation processes, including phthalate transformation, and the rates of degradation were closely correlated with the rates of methanogenesis.

Conclusions

Our modelling of the degradation of MSW under landfill conditions shows that the waste should preferably be divided into two fractions, readily degradable and recalcitrant waste, in order to account for the delay in hydrolysis and methanogenesis observed as related to acidogenesis. This strategy allowed us to show that the degradation of the readily degradable waste fraction generated conditions that inhibited further degradation of the waste, i.e. primarily hydrolysis but also methanogenesis. This suggests that the inhibitory period is likely to be longer for MSW with a high ratio of readily degradable to recalcitrant waste fractions. This hypothesis was confirmed by modelling MSW where the readily degradable waste had been initially eliminated by aeration. In this case, the ratio was minimal and, consequently, the methanogenesis commenced immediately after termination of the aeration period, leading to depletion of the readily degradable waste fraction. The inhibition is most likely caused by a web of complex and interacting mechanisms, but according to this study it is directly and/or indirectly related to low pH, i.e. $\text{pH} < 6$. The patterns of the modelled transformations of DEP and MEP confirmed the general features of the 1-D model. The modelled profiles throughout the vertical coordinate of the studied reactors suggest that degradation of MSW in fullscale landfills should be enhanced by the application of methanogenic leachate to the top layer of newly deposited MSW to avoid acid generation, and thus inhibition and subsequent delay of efficient methanogenic degradation of the bulk waste.

Acknowledgements

The reviewers are gratefully acknowledged for their valuable comments on the text. This work was supported in part by the INCO-Copernicus-2 Program (grant ICA2-CT-2001–10001). The generous support of Vasily A. Vavilin and Susanne Jonsson by the Swedish Foundation for International Cooperation in Research and Higher Education (grant nos. KG2003–4513 and KU2003–4056) is greatly appreciated.

References

Barlaz MA, Schaefer DM & Ham RK (1989) Bacterial population development and chemical characteristics of refuse decomposition in a simulated sanitary landfill. Appl. Environ. Microbiol. 55: 55–65

Batstone DJ., Keller J, Angelidaki I, Kalyuzhnyi SV, Pavlostathis SG, Rozzi A, Sanders WTM, Siegrist H & Vavilin VA (2002) The IWA anaerobic digestion model No.1 (ADM1). Wat. Sci. Technol. 45(10), 65–73

Christensen TH & Kjeldsen P. (1989) Basic biochemical processes in landfills. In: Christensen TH (Ed) Sanitary Landfilling: Process, Technology and Environmental Impact, (pp 29–49). Academic Press, London

Chynoweth DP & Pullammanappallil P (1996) Anaerobic digestion of municipal solid wastes. In: Palmisano AC & Barlaz MA (Eds) Microbiology of Solid Waste, (pp 71–13). CRS Press, Boca Raton, FL

Ejlertsson J, Houwen FP & Svensson BH (1996a) Anaerobic degradation of diethyl phthalate and phthalic acid during incubation of municipal solid waste from a biogas digester. Swedish J. Agric. Res. 26: 53–59

Ejlertsson J., Houwen FP & Svensson BH (1996b) Anaerobic degradation of phthalic acid esters during digestion of municipal solid waste under landfilling conditions. Biodegradation 7: 345–352

Ejlertsson J, Karlsson A, Lagerkvist Hjertberg A T & Svensson BH (2003) Effect of codisposal of wastes containing organic pollutants with municipal solid waste – a landfill simulation reactor study. Adv. Environ. Res. 7: 949–960

Gavala HN, Alatriste-Monragon F, Iranpour R & Ahring BK (2003) Biodegradation of phthalate esters during the mesophylic anaerobic digestion of sludge. Chemosphere 52: 673–682

Jonsson S, Ejlertsson J & Svensson BH (2003a) Behavior of mono- and diesters of o-phthalic acid in leachates released during digestion of municipal solid waste under landfill conditions. Adv. Environ. Res. 7: 429–440

Jonsson S, Ejlertsson J, Ledin A, Mersiowsky I & Svensson BH (2003b) Behaviour of mono- and diesters from o-phthalic acid in leachates from different European landfills. Water Res. 37: 609–617

Jonsson S, Ejlertsson J & Svensson BH (2003c) Transformation of phthalates in young landfill cells. Waste Management 23: 641–651

Jonsson S & Baun A (2003) Toxicity of mono- and diesters of o-phthalic esters to a crustacean, a green alga, and a bacterium. Environ. Toxicol. Chem. 22(12), 3037–3043

Lagerkvist A & Chen H (1992) Control of anaerobic degradation of MSW by enzyme addition. Proc. Int. Symp on Anaerobic Digestion of Solid Waste, IAWPRC, Venice, Italy. (pp 75–84)

Lagerkvist A (2003) (Ed) Landfill Technology Technical Report 2003:15, Luleå University of Technology. Dept. of Env. Engineer, Div. Waste Science and Technology, pp 10–32

Pohland FG, Cross WH & King LW (1992) Codisposal of disposable diapers with shredded municipal refuse in simulated landfills. Proc. Int. Symp on Anaerobic Digestion of Solid Waste, IAWPRC, Venice, Italy. pp 269–283

Saeger VW & Tucker ES (1973) Pthalate esters undergo ready biodegradation. Plastics Engineering 29: 46–49

Staples CH, Peterson DR, Parkerton TF & Adams WJ (1997) The environmental fate of phthalate esters: literature review. Chemosphere 35: 667–749

Stegmann R (1981) Beschreibung eines Verfahrens zur Untersuchung anaerober Umsetzungsprozesse von Festen Abfallstoffen im Labormab-stab. Mull und Abfall 2

ten Brummeler E, Horbach HCJM & Koster IW (1991) Dry anaerobic batch digestion of the organic fraction of municipal solid waste. J.Chem. Tech. Biotechnol. 50: 191–209

Vavilin VA, Rytov SV, Pavlostathis SG & Barlaz MA (2003) Distributed model of solid waste anaerobic digestion: effects of leachate recirculation and pH adjustment. Biotech. Bioengn. 81: 66–73

Vavilin VA (2003) Landfill as an excitable media. Conf. Proc: Workshop on Sustainable Landfill Management (pp 51–60) 3–5 Dec 2003, Chennai, India. Allied Publisher Pvt Limited, New Delhi

Vavilin VA, Lokshina LYa, Jokela JPY & Rintala JA (2004) Modelling solid waste decomposition. Biores. Technol. 94: 69–81

Wolfe NL, Steen WC & Burns LA (1980) Phthalate ester hydrolysis: Linear free energy relationships. Chemosphere 9: 403–408